

Planar and Spherical Near-Field Range Comparison with -60 dB Residual Error Level

Allen Newell, Greg Hindman
Nearfield Systems Inc.
19730 Magellan Drive
Torrance, CA 90502

ABSTRACT

Comparisons of the far-field results from two different ranges are a useful complement to the detailed 18 term uncertainty analysis procedure. Such comparisons can verify that the individual estimates of uncertainty for each range are reliable or indicate whether they are either too conservative or too optimistic. Such a comparison has recently been completed using planar and spherical near-field ranges at Nearfield Systems Inc. The test antenna was a mechanically and electrically stable slotted waveguide array with relatively low side lobes and cross polarization and a gain of approximately 35 dBi.

The accuracies of both ranges were improved by testing for, and where appropriate, applying small corrections to the measured data for some of the individual 18 terms. The corrections reduce, but do not eliminate the errors for the selected terms and do not change the basic near-to-far field transformations or probe correction processes. The corrections considered were for bias error leakage, multiple reflections, rotary joint variations and spherical range alignment. Room scattering for the spherical measurements was evaluated using the MARS processing developed by NSI.

The final results showed a peak equivalent error signal level in the side lobe region of approximately -60 dB for both main and cross component patterns for angles of up to 80 degrees off-axis.

Keywords: Antenna Measurements, Error Analysis, Near-Field Measurements, Range Comparison.

1.0 Introduction

The quality of an antenna measurement ranges is traditionally given in terms of the stray signal level or error signal that represents its departure from ideal conditions. For far-field, compact ranges and anechoic chambers, this signal is usually estimated by measuring the departure of the incident field in a “quiet zone” from an ideal singly polarized plane wave. Stray signals from ground reflections, chamber scattering, edge diffraction or feed interference will produce periodic variations in the field and the level of the stray signal relative to the

desired plane wave can be inferred from the amplitude of the ripple it produces. In addition to periodic variations, curvature in the amplitude and phase of the field is caused by the finite size of ranges and reflectors used in compact ranges. It is generally assumed that the departure from an ideal plane wave is the major source of error in these ranges and the stray signal level is therefore used to represent the total uncertainty in the range. Ranges with a stray signal level of -40 dB over the operating frequency are considered high quality and careful attention to design and construction of the ranges are required to achieve this level.

The stray signal level is also used to specify the quality of a near-field antenna range, and in this application it is generally referred to as the “error signal level”. It also represents the estimated level of one or more sources of error that contribute to uncertainty in the antenna parameters determined from near-field measurements. Some error sources are not due to an actual stray signal but they can be represented as an equivalent error signal by converting uncertainties in dB to error signal using the relations

$$ERROR / Signal = E / S = 20 * \log \left[10^{\left(\frac{\Delta_{dB}}{20}\right)} - 1 \right] \quad (1)$$

$$Error \text{ in dB} = \Delta_{dB} = 20 * \log \left[1 + 10^{\left(\frac{E/S}{20}\right)} \right]$$

The total estimated uncertainties in antenna parameters such as gain, side lobe level, cross polarization level, and beam pointing are derived using a procedure referred to as the NIST 18 Term Error Analysis¹. The contributions for each of the 18 terms are estimated using a combination of analysis, self comparison measurements and simulation and then they are combined using an RSS process. For example, multiple reflections between the AUT and the probe can produce errors in all of the far-field parameters, and it is evaluated in planar measurements by acquiring data at a sequence of Z-distances in steps of lambda/8. The far-field patterns for each data set are calculated and then averaged to reduce the effect of the multiple

reflections. Comparing a single far-field to the average gives an estimate of this error source.

Another result of identifying and estimating the individual measurement errors has been the development of correction techniques for some of the terms. These techniques use either additional information about the measurement system such as a Z-position error map or additional near-field data to reduce the uncertainty of individual terms.

The current measurement was undertaken to test and apply existing and newly developed correction techniques in planar and spherical near-field measurements and to quantify the reduction in uncertainties in far-field parameters. For this measurement, the focus was on side lobe level and gain measurements were not performed.

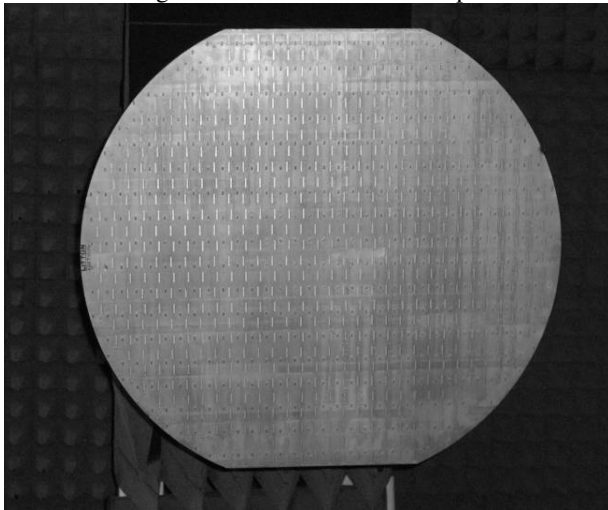


Figure 1 Slotted waveguide array used in the range comparison measurements.

The antenna under test (AUT) was a fixed beam array operating at 9.375 GHz shown in Figure 1. It was mechanically very stable and could be moved from one range to another and realigned precisely. The goal was to perform measurements on the two ranges as accurately as possible, apply appropriate measurement corrections and demonstrate typical accuracy for near-field ranges.

2.0 Initial Measurement System Adjustments

To insure accurate measurements and comparisons on both ranges, the following steps were taken.

Alignment. When patterns from different ranges are compared, it is very important to align the rotation of the AUT about the X, Y and Z axes to be the same on both ranges. The far-field software generally provides a means to adjust the azimuth, elevation and tilt angle zeroes before plotting and comparing patterns, but for precise

comparison the rotations about the Z-axis must be as identical as possible. This physical rotation will change the polarization vectors, but it will also rotate the pattern about the Z-axis so that the cuts from the two ranges will not be along the same lines in the AUT coordinate system. It is not possible to adjust the zeroes of all three angles in the software and produce identical cuts for two different ranges. This can be seen from the equations relating the AZ/EL angles to the Theta/Phi angles,

$$\sin(AZ) = \frac{\sin(\theta)\cos(\phi)}{\sqrt{1 - (\sin(\theta)\sin(\phi))^2}} \quad (2)$$

For an Elevation cut, ϕ is equal to 90 degrees plus the rotation of the AUT about the Z-axis and θ is approximately equal to the EL angle. If the AUT for planar measurements is rotated about the Z-axis by only 0.1 degrees compared to the spherical orientation, the AZ angle will be shifted by almost -0.2 degrees for EL = +60 degrees and by +0.2 degrees for EL = -60 degrees. In these regions the nulls and lobes are very sharp and this offset will produce noticeable pattern differences. To minimize this alignment error, the Z-axis rotation of the AUT on both ranges was set using a precision level and then the planar alignment was fine tuned to match the spherical alignment using the resulting tilt angle and 2D pattern comparisons. For the final measurements, the Z-rotation on the two ranges agreed to within 0.02 degrees.

RF Signal-to-Noise The error signal level derived from the pattern comparisons cannot be any lower than the far-field noise-to-signal ratio on each range. This noise level is determined by the near-field RF noise-to-signal ratio, the stability of the RF system and random position errors. The input RF signal and receiver averaging were set to achieve a signal-to-noise ratio of at least +75 dB for both ranges and the far-field noise level was estimated by repeating the measurements on each range a number of times, averaging the resulting patterns and comparing to a single measurement. The result for the spherical range showed a random error in the side lobe region of -80 dB as shown in Figure 2. The corresponding noise level for the planar measurements was -70 dB. The higher level in the main beam region of Figure 2 is due to small beam peak angular shifts caused by drift in the RF and mechanical systems over the measurement time. The double peaked difference pattern is characteristic of a beam peak shift of only 0.02 degrees in this case. Similar differences occur in the comparison of patterns from the two ranges and small manual adjustments can be applied to the beam peak angles to reduce this difference. In a

sense, this is one correction for the effect of measurement drift.

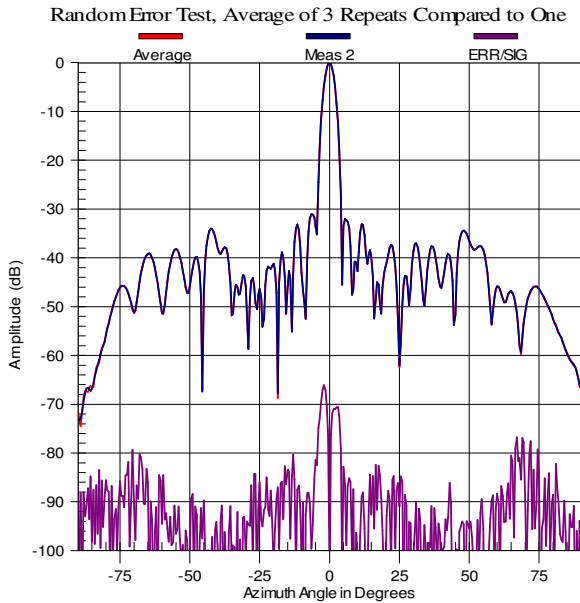


Figure 2 Random error for spherical estimated from comparison of three repeat measurements.

Data Point Spacing Aliasing errors will occur for both spherical and planar measurements if the data point spacing is not small enough to sample the highest spatial frequency components in the measured data. The RF frequency and the AUT size and position in the measurement sphere prescribe a theoretical allowable spacing but other factors can require a smaller spacing. In the planar measurements, multiple reflections between the AUT and the probe can be modulated by the periodic structure of an array antenna producing “artificial” evanescent modes in the far-field pattern and requiring spacing less than $\lambda/2$. This was the case for this antenna as determined by preliminary data and so a spacing of $\lambda/4$ was used for all planar measurements. For the spherical measurements, both probe and room scattering can produce higher spatial frequencies in the data and preliminary tests indicated that 1.0 degree spacing should be used rather than the theoretical 1.5 degrees to prevent aliasing errors.

Truncation The effect of truncation on the planar data was reduced by using a scan area of 100 X 100 inches and a Z distance of 3 inches. This should give reliable far-field patterns to at least 80 degrees off axis.

3.0 Correction Techniques for Some Error Terms

The development of analysis and measurements to estimate the individual error terms has led to the

development of correction techniques for some of the terms that in some cases can significantly reduce the uncertainty in far-field results. These are summarized in Table 1. In addition to the listed items, correction for the gain, pattern and polarization of the probe are included as a standard part of the data processing. A network correction can also be applied for dual port probes to account for different transmission lines between the two ports and the receiver. These will not be considered in detail here since they are routinely applied and well understood.

Table 1 Near-Field Corrections.

Correction Technique	Far-Field Parameters Affected
Multiple Reflections Planar and Spherical	Gain, Side lobe, Cross Pol, Pointing
AUT Alignment Planar and Spherical	Pointing Pattern comparisons
X, Y and Z Position Errors Planar	Gain, Side lobe, Cross Pol, Pointing
Rotator Alignment and position Errors Spherical	Gain, Side lobe, Cross Pol, Pointing
Drift Correction Planar and Spherical	Gain, Pointing
Flexing Cable Planar	Gain, Side lobe, Cross Pol, Pointing
Probe Rotary Joint Spherical	Gain, Side lobe, Cross Pol, Pointing
Room Scattering Spherical	Gain, Side lobe, Cross Pol, Pointing
Impedance Mismatch Planar and Spherical	Gain
Bias Error Leakage Planar	Gain, Cross Pol, Pointing

Multiple Reflections Planar and Spherical. To correct for multiple reflections between the AUT and probe, complete near-field measurements are taken at a series of Z-positions separated by $\lambda/8$. The far-fields are calculated for each and then averaged.

AUT alignment Planar and Spherical. When the AUT is not precisely aligned to the reference coordinate system, the patterns can be rotated mathematically. Vector components and or coordinate angles may change for some rotations and this correction must be used carefully.

Position Errors Correction Planar and Spherical. This correction can take different forms. The precise position of the probe can be monitored during the measurement process with laser optics and the probe can be moved in X, Y and Z to correct for deviations from the ideal surface

and raster coordinates. The probe motion can also be recorded with an optical system and the information stored in the measurement computer. This information can be used to mechanically correct for the position errors during measurements or applied as an approximate mathematical correction during processing². The mechanical Z correction was used on the planar measurements.

Rotator Alignment for Spherical. This is a special case of position error correction. The orthogonality and intersection of the theta and phi axes and the coincidence of the phi and probe polarization axes can be checked by measuring and comparing near-field cuts at $\theta = 0$ and 180 degrees. The misalignment can be corrected by adjustments of the mechanical system or an approximate mathematical correction can be applied for small deviations.

Drift for Planar and Spherical Thermal drift during measurements can cause changes in the transmission lines and electronic components as well as the alignment of the AUT. These can be corrected by periodically returning to one or more reference point on the measurement grid and recording the amplitude and phase of the probe output as described in the NSI developed MTI technique. Numerical correction is then applied to the measured data³.

Flexing Cable Correction for Planar. The RF cables connecting the moving probe to the source or receiver will introduce some amplitude and phase variation as it is moved. Like the position correction, the cable variations can be measured and stored for future correction or in some cases the variations and corrections are recorded and applied^{4 5} during measurements.

Probe Rotary Joint Correction for Spherical. The rotary joints associated with the theta and phi rotators produce an effect similar to the flexing cable in planar measurements and can be treated in a similar way. They produce small position variations as a function of theta and phi that usually have little effect on the far-field patterns. The rotary joint used for the probe polarization can have a more serious affect since it is rotated to just two positions and all of the data for one component has the same error applied. A correction can be obtained from the measured data by comparing the amplitudes and phases of the two components at (θ, ϕ) coordinates, (0,0), (0,90), (0,180), (0,270), (0,360). From knowledge of the AUT and probe polarizations we can identify the points where the amplitudes should be identical and the phases should be either identical or 180 degrees different. From the measured values at these points, a constant correction can be determined and applied to all the data for one

component. This correction is more important at high frequencies where rotary joints may not be as accurate.

Impedance Mismatch Correction. To obtain gain, EIRP or saturating flux density results from near-field data, a gain standard is required and one or more transmission lines must be moved from the AUT or probe to the gain standard. The different power transfer between the transmission line and the antennas can be accounted for by measuring the complex impedance of each device and applying a calculated correction. This correction does not affect relative patterns, polarization or beam pointing.

Bias Error Leakage for Planar. The detection and conversion of the RF signals to real and imaginary or amplitude and phase components in the receivers introduces a small bias error that produces a very small constant signal on the recorded amplitude and phases of the near-field pattern. This signal may be 50 to 100 dB below the peak near-field amplitude, but in the FFT processing of the data for planar measurements, the leakage signal is summed coherently in the on-axis direction. It can produce a noticeable distortion in the main beam region if the measurement area is much larger than the AUT area. The amplitude and phase of the bias error can be determined from the data without additional measurements⁶. Scripts have been developed to use the measured data at the extremes of the measurement area where the amplitude is small. In this region, the sum of the data will converge to the constant bias error and it can then be subtracted from the measured data⁷.

Bias error leakage has no effect on spherical data since a constant signal over the sphere does not produce or modify any of the calculated spherical modes.

Room Scattering Correction for Spherical. Scattering from structures and absorber in a planar near-field range introduces an error that is generally small for directive antennas. It is also difficult to estimate this error, partly because it is small and because the procedure is demanding and time consuming. The AUT and probe must be translated together in a combination of X, Y and Z movements while maintaining precise angular alignment. The translations should be at least multiple wavelengths in dimension and this generally means that the AUT must be realigned in the new position. Comparison of the patterns from the two locations provides an estimate of the room scattering but it is difficult to distinguish from alignment differences, probe/AUT multiple reflections and system drift. There is no practical way to correct for room scattering in planar measurements since this would require multiple repositioning of the AUT and probe.

The room scattering effect for spherical measurements can be more severe when low gain AUT's are being measured. Techniques have been developed⁸ for the spherical measurements that can reduce the effect of room scattering for some situations. The MARS technique developed by NSI uses the following measurement and processing steps and a similar procedure is used in another technique⁹. The AUT is oriented with its nominal phase center translated from the origin of the spherical coordinate system by at least 2 wavelengths. The spherical near-field data is over sampled by a factor of two and the usual near-field data acquired. Graphics produced during the subsequent processing will indicate if the over sampling is sufficient or excessive. The actual location of the AUT phase center is determined as the first step in the processing by fitting the far-field phase patterns in the region of the main beam. The far-field pattern is calculated from the measured data and a phase correction is applied to effectively translate the AUT so its phase center is at the origin. This translated far-field pattern is copied to the near-field and replaces the original measured data. The new data is again processed through the spherical transform software and a filter is applied to remove the higher order modes that are inconsistent with the AUT physical dimensions. Room scattering that is contained in these higher order modes is therefore eliminated from the final results. Room scattering that is contained in the lower order modes will not be removed and remains in the far-field pattern. Numerous tests have shown that for low and medium gain antennas, room scattering effects can be reduced by approximately 10 dB with this process. When the room scattering levels are very small, such as for a directive AUT in a reasonably good chamber, the improvement may be small because the error level is already so low.

4.0 Planar/Spherical Comparison Measurements

In any given measurement, the desired level for the total estimated error signal level and the impact of each term will generally dictate whether or not to apply a given correction. In some cases the change in the far-field parameters can be measured by comparing the results with and without the correction. The pattern subtraction technique illustrated in Figure 2 is used but in this case the "error signal level" is used to quantify the change produced by the correction. A very low level indicates that the correction has little if any effect on the results and can be neglected in similar measurements.

Once the correction is applied, the error signal level should be lower, but additional tests may be necessary to quantify the improvement. This was one of the motivations for the following measurement comparison. The same antenna was measured on both the planar and

spherical ranges. Each correction was tested on the appropriate data to determine if significant improvement was possible. The patterns were compared at different stages in the process, and an error signal level was determined that represented the difference between the two ranges. As corrections were applied, the error signal was reduced and this was used to estimate the improvement due to the correction. The final level then represents the total estimated uncertainty for each range. This final level is potentially lower than the estimate arrived at using the 18 term error analysis since some of those tests may not be sensitive enough to establish a lower bound.

With the initial alignment and settings on both ranges, the first comparisons indicated a peak difference level of approximately -40 dB as shown in Figure 3.

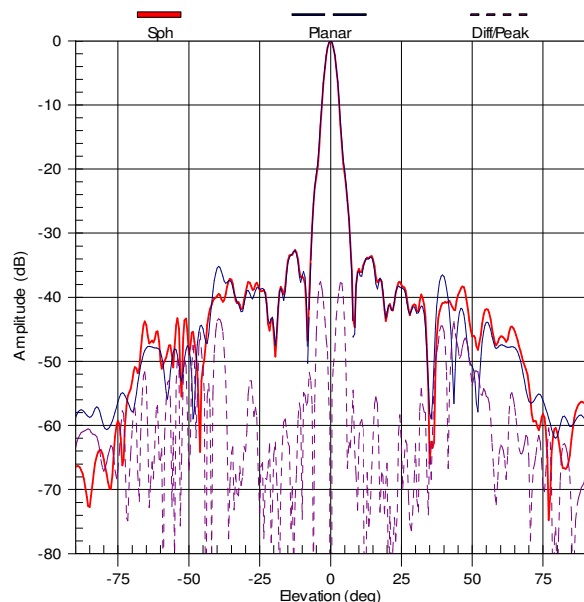


Figure 3 Initial comparison between planar and spherical measurements before precise alignment or corrections applied.

The main beam difference is due primarily to bias error leakage in the planar measurements. This produces some distortion near the peak of the main beam as shown in Figure 4. The five cuts in Figure 4 are from multiple reflection data taken at slightly different Z distances. The constant leakage signal has a different phase relationships to the peak far-field at different Z positions and therefore causes different distortion. This error can be reduced by repeating the measurement with increased signal or higher averaging. Existing data can be corrected by applying a leakage correction where the amplitude and phase of the leakage signal is determined from the measured data and then subtracted before calculating the far-field. Both

corrections were applied in the current measurements. With these correction, the difference peak was approximately -50 dB.

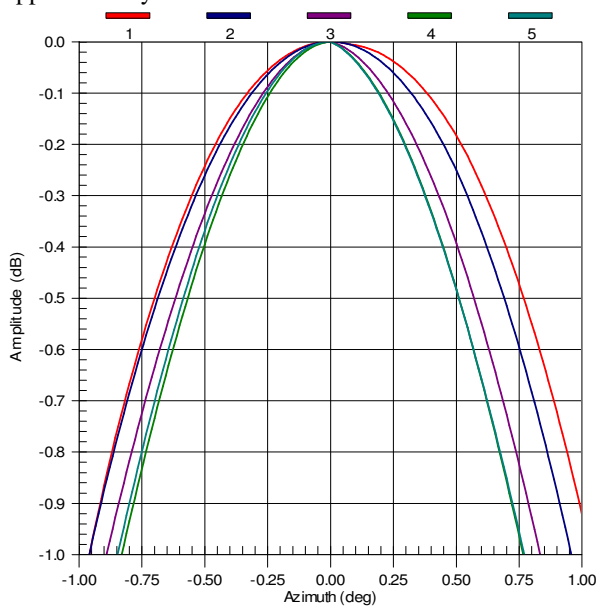


Figure 4 Main beam distortions in planar far-field results caused by bias error leakage for five different Z-positions.

Multiple reflection processing was then applied to the planar measurements where data at four or more Z distances was averaged in the far-field. Multiple reflection, rotary joint and room scattering corrections were tested on the spherical data, but the improvements were all near the noise level. The narrow beam and low

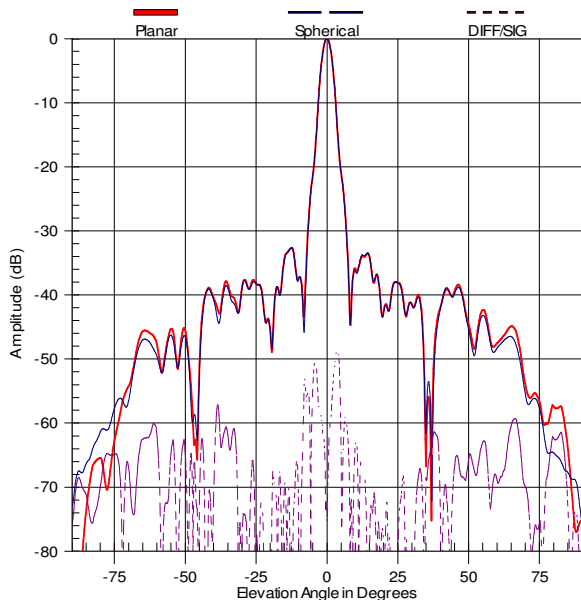


Figure 5 Final comparison of main component far-field pattern results between planar and spherical ranges.

side lobes of the AUT along with the measurement radius of nearly 2 m greatly reduced scattering interference in the data. Typical results for the main component pattern comparisons are shown in Figures 5. The probable cause for the double peaks in the main beam region is cable phase variations as the probe moves in the Y-direction. Phase variations of only about 2 degrees could produce the observed difference. This error could be reduced by calibrating the cable, but since this has virtually no effect on gain, directivity cross polarization or side lobe level, it is seldom necessary.

5.0 Summary

Comparison measurements between a planar and spherical near-field range along with procedures to estimate and correct measurement uncertainties have demonstrated that both ranges are capable of achieving an equivalent error signal level of -60 dB in the side lobe region and -50 dB in the main beam region. Both ranges are typical industrial type facilities and similar performance should be expected when each potential error source is carefully considered and steps are taken to reduce or correct their effect on far-field results.

8. REFERENCES

- ¹ A. C. Newell, Error analysis techniques for planar near-field measurements, IEEE Trans. Antennas & Propagation, AP-36, p. 581, 1988
- ² Wittmann, R.C., Spherical near-field scanning: determining the incident field near a rotatable probe, IEEE Antenna Propagation Society Symposium Digest, 7-11 May, Vol.1, pp.224-227, Dallas, TX, 1990
- ³ Hindman, G., Slater, D, Thermal Error Corrections in Near-Field Measurements, AMTA Proceedings, Oct. 1995.
- ⁴ Hess, D.W., Principle of the three-cable method for compensation of cable variations, AMTA Symposium Digest, pp.10-26 – 10-31, Columbus, OH, 1992.
- ⁵ Tuovinen, J., Lehto, A., Raisanen, A., A new method for correcting phase errors caused by flexing of cables in antenna measurements, IEEE Transactions, AP-39 No.6, June 1991..
- ⁶ Rousseau, P. R., “An algorithm to reduce errors in planar near-field measurement data, AMTA Proceedings, Oct. 1999, pp 269-271.
- ⁷ Newell, A. C., Guerrieri, J., MacReynolds, K., Methods to estimate and reduce leakage bias errors in planar near-field antenna measurements, AMTA Proceedings, Oct. 2002
- ⁸ Hindman, G., Newell, A.C., Reflection suppression in a large spherical near-field range, AMTA Symposium Digest, pp.270-275, Newport, RI, 2005
- ⁹ Hess, D.W. The *IsoFilter*[™] technique: isolating an individual radiator from spherical near-field data measured

in a contaminated environment, Postdeadline Submissions,
AMTA Symposium, Austin, TX, 2006